

Original Paper

All solid-state Li-ion batteries based on intercalation electrodes and poly (ethylene oxide)-LiX electrolytes

Y. Liu^a, Y. Ono^b, T. Matsumura^b, A. Hirano^b, T. Ichikawa^b, N. Imanishi^b and Y. Takeda^b
(^a Satellite Venture Business Laboratory, ^b Department of Chemistry for Materials)

(Received September 20, 2005)

Abstract

All-solid state rechargeable Li-ion batteries based on poly (ethylene oxide) electrolytes are promising power sources for large application such as electric vehicles (EV), which could be likely to require safety and reliability as well as high energy density and long cycle life. However, so far, state-of-the-art electrode materials are limited by the performance factors such as electrochemical instability to lithium insertion/extraction, particularly at the solid/solid interface between the electrodes and the PEO electrolytes. The efforts on conquering above dilemma have been carried out over several decades. Recently, we developed novel or modified insertion type electrodes, which demonstrate good electrochemical behavior with the PEO electrolytes at the elevated temperature. In this paper, preparation and characterization of the electrodes proposed are presented and discussed in detail.

Key words: Power sources; Rechargeable lithium ion batteries; All solid-state PEO electrolytes; Insertion electrodes; Energy density; Thermal safety.

1. Introduction

Solid-state rechargeable batteries, especially, lithium ion batteries, are principle and promising power sources for a wide variety of electronics. PEO electrolyte formed by dissolving a lithium salt in a host poly (ethylene oxide) (PEO) shows high ionic conductivity ($\sigma > 10^{-4}$ S cm⁻¹) at the elevated temperature. Rechargeable lithium batteries based on the PEO electrolytes have been proposed to overcome low energy density of previously used batteries such as lead acid and nickel metal hydride and to improve safety of conventional lithium-ion batteries with an inflammable liquid electrolyte [1]. The PEO type cells have several benefits such as feasible design and ductile morphology which can absorb volume change for Li insertion/extraction in electrodes. Although the high temperature limitation (>60 °C) of the PEO cell is a drawback for applications in the consumer electronic market, it is probably an advantage for numerous other applications such as for electric vehicles (EV). For these large size batteries in EV, safety and reliability are the most important issues. Previously developed lithium polymer batteries contain lithium metal anodes. A lithium battery incident at Los Angeles International Airport on 28 April, 1999 suggests that safety of a lithium battery with a large amount of lithium metal is questionable [2]. In addition, an improvement on the ionic conductivity and Li⁺ transfer number has to be done to achieve a relatively high charge rate. Therefore, so far, research has been extensively concentrated on two major points such as 1) the improvement of ionic conductivity of PEO-LiX complex at the relatively low temperature and 2) searching for novel or modified electrodes which can deliver good interfacial compatibility with the solid PEO electrolytes. By this motivation, in the anode side, researchers have undertaken to replace the lithium metal by a safer one, such as insertion anode, with a high capacity and an excellent reversibility. Lithium-insertion hosts such as carbon, Li-alloy and Li-M-O are promising alternative anodes [3, 4]. Unfortunately, carbon still cannot be adopted successfully with the PEO electrolytes due to the interfacial incompatibility, regardless of its wonderful electrochemical manners in the liquid system. On the other hand, some Li-M-O materials, e.g., spinel Li₄Ti₅O₁₂, demonstrate zero-strain effects for Li-insertion, resulting in long cycling life with the solid PEO electrolytes. However, relatively low capacity and high Li reactive potentials of lithium titanates make them incomparable in the energy density. On the other hand, in the cathode side, the most common cathodes such as LiCoO₂, LiNiO₂, LiCo_xNi_{1-x}O₂, and LiMn₂O₄ all suffer from side reaction with PEO electrolytes and detrimental phase transitions above 70 °C that inevitably cause to capacity loss and fade while being oxidized at a high potential. Meanwhile, state-of-the-art electrode materials are limited by the performance factors such as electrochemical instability to

lithium insertion/extraction, particularly at the interface between the electrodes and the PEO electrolytes. Therefore, development in the electrode materials in associated with the PEO electrolytes would be urgent.

2. Experimental

2.1 Materials preparations

To produce the hexagonal lithium transition-metal nitrides, a given ratio of Li_3N and powders of transition metals was homogeneously mixed in an Ar atmosphere. The mixture was pressed into a tablet with 8 mm in diameter and 5-8 mm in thickness and heated at 700 °C for 12 h under N_2 stream with heating rate of 35 °C min^{-1} . The reactions were allowed cool down to room temperature normally. For the compounds containing Fe, the heating temperature was increased to 800 °C. The resulting products were ground in a glove box and further treated by high-energy mechanical milling (HEMM) at a rotational speed of 500 rpm for 20 h. The modification for the graphitic carbon was as follows: a given amount of graphitic carbon was dried under vacuum at high temperature, and then was mixed with metallic lithium and selected organic solvent under a certain ratio under inert atmosphere. The mixture was treated by high energy mechanical milling under inert atmosphere. The milled product was further dried under high temperature to entirely remove the residual organic solvent. Ultrafine SnSb alloy powder (particle size < 0.2 μm) was prepared by chemical precipitation from aqueous solutions containing the reductive agent NaBH_4 and respective metallic salts in the presence of complexants such as citrates. The Co_3O_4 powder (< 2 μm) was obtained by a thermal decomposition of CoCO_3 at 800 °C in air. $\text{LiNi}_{0.8}\text{Co}_{0.2}\text{O}_2$ (ca. 10 μm) was prepared from the mixture of Li_2O_2 (Aldrich) and $(\text{Ni}_{0.8}\text{Co}_{0.2})\text{O}$ precursor which was obtained from the decomposition of the hydroxide at 300 °C for 1 h. The mixture was heated at 700 °C for 24 h under O_2 gas flow. LiFePO_4 and LiFePO_4/C (PVC as carbon sources) was prepared as follows: a certain amount of Li_2CO_3 , poly (vinyl chloride) (PVC), $\text{NH}_4\text{H}_2\text{PO}_4$ and FeC_2O_4 was homogeneously mixed by the aid of THF. The mixture was heated firstly at 350 °C for 3-6 h and smashed at room temperature. The smashed products were further heated at 700-900 °C for 16 h under Ar. The final samples were ground and sieved. Powder X-ray diffraction (XRD) patterns were obtained using automated powder diffractometer with $\text{Cu K}\alpha$ radiation (Rotaflex RU-200B, Rigaku-denki Corporation). The morphological performance of the materials was characterized with scanning electron microscopy (SEM) and Electron Probe Micro-Analysis (EPMA).

2.2 PEO Electrolytes and cathode film

PEO electrolytes (Li/O ratio: 1/18) were prepared under a casting technique. All the procedure was protected by Ar atmosphere in the glove box. A given weight of PEO (MW = 6×10^5) and $\text{LiN}(\text{CF}_3\text{SO}_2)_2$ was dissolved completely in anhydrous acetonitrile (AN). BaTiO_3 (ca. 0.1 μm) was dispersed homogeneously in the solution as filler. After strong stirring overnight the viscous solution was cast into a Teflon dish. After AN was slowly and completely evaporated under a N_2 flow, the obtained film was further dried at 90 °C under vacuum at least 8 h. The conductivities of the composite polymer electrolyte were observed as high as $1.7 \times 10^{-3} \text{ S cm}^{-1}$ at 80 °C and $0.82 \times 10^{-3} \text{ S cm}^{-1}$ at 65 °C and the decomposition potential was estimated to be more than 4.2 V (vs. Li/Li^+). The cathode electrode consisting of 52 wt.% active hosts (LiFePO_4 or $\text{LiNi}_{0.8}\text{Co}_{0.2}\text{O}_2$), 10 wt.% acetylene black (AB) and 38 wt.% PEO- $\text{LiN}(\text{CF}_3\text{SO}_2)_2$ (Li/O ratio: 1/18) were prepared by the casting method similar to PEO film and the thickness was about 200 μm .

2.3 Anode preparations

For all the electrodes, a given weight of the electrode components was homogeneously mixed in an agate mortar in a glove box and further pressed onto a 300-mesh stainless steel grid, which served as a current collector. The geometric area of the electrodes was 0.55 cm^2 , and the typical thickness was 100~160 μm .

2.4 Electrochemical and thermal stability (DSC) measurements

To evaluate the electrochemical properties of the electrodes, a half-cell containing Li metal as the counter and $\text{LiPF}_6 / \text{EC} + \text{DMC}$ (Ethylene carbonate plus diethyl carbonate as 1:1 in volume) electrolytes (in case of the cells with the liquid electrolytes) was used. Basically all the three layers, including test electrode, separator and Li metal, were stacked in a 2025 coin type cell in a glove box. For the cells based on the PEO electrolyte, the separator was replaced by the PEO film, which also served as electrolyte. The full solid-state cell was constituted by replacing lithium metal with the cathode films. A small constant pressure was kept inside cells by means of the Ni foam as filler. Before the electrochemical test, the PEO based cells were preheated for 2 hrs at a temperature of 75 °C. Unless stated elsewhere, the cells were carried out at a constant current density of 0.1-0.15 mA cm^{-2} . The rest time between charge and discharge was 1 min.

3. Results and discussion

3.1 Anodes

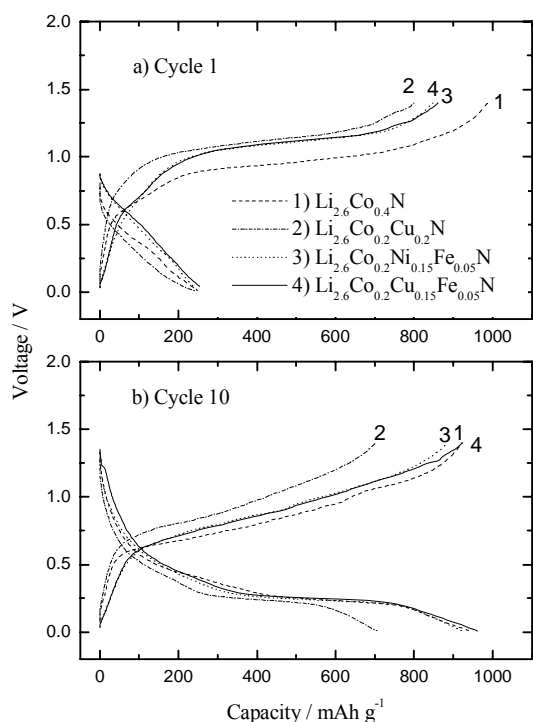


Fig.1. Charge and discharge curves of the electrodes based on lithium transition-metal nitrides at the first and tenth cycle, voltage cutoff: 0-1.4 V, vs. Li/Li^+ . Electrode composition: 20 wt.% AB, 70 wt.% lithium metal nitrides and 10 wt.% PVDF.

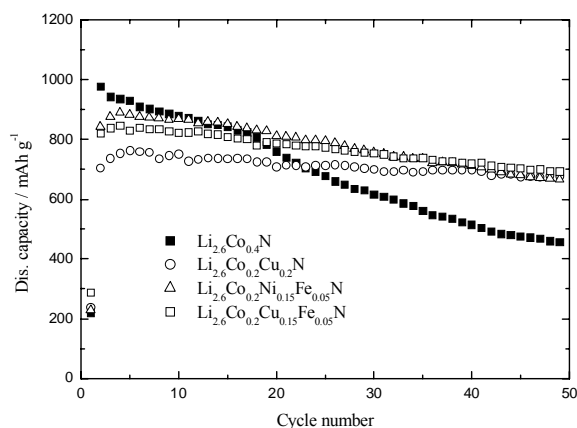


Fig.2. Cycling performance of the electrodes based on lithium transition-metal nitrides. Electrode compositions are the same as in Fig. 1.

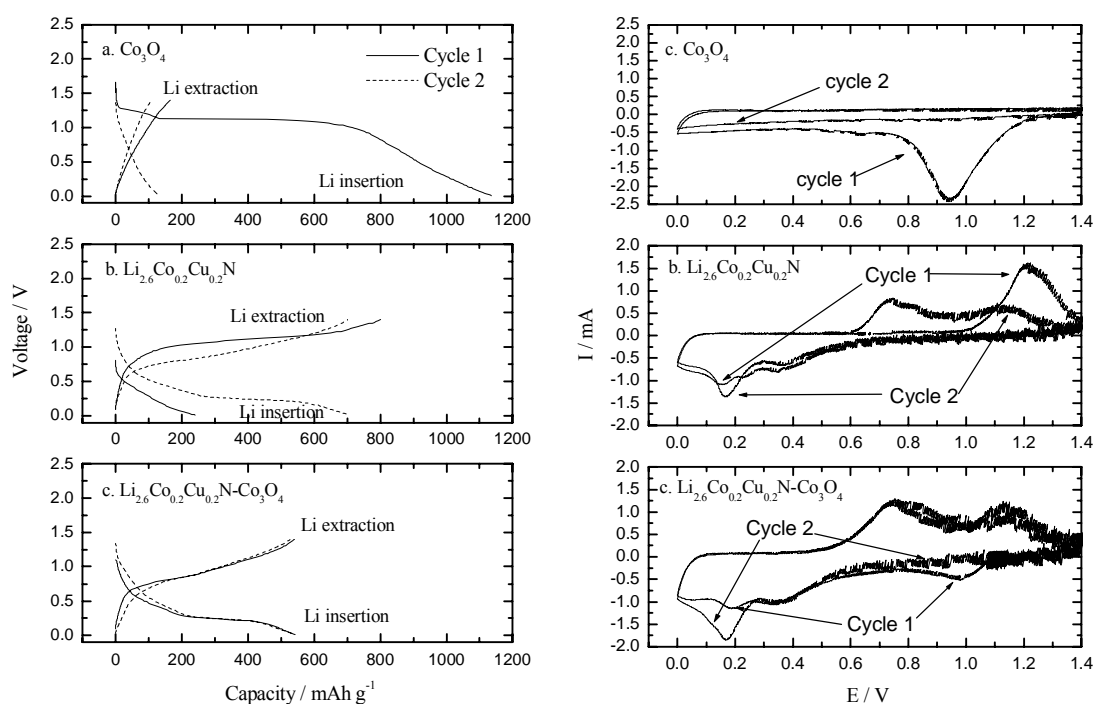
under a potential of 0-1.4 V with liquid electrolytes at room temperature. The Co_3O_4 electrode has a large insertion capacity of 1150 mAh g^{-1} along with a potential plateau of about 1.05 V in the first cycle. However, its capacity retention in the subsequent cycle shown in Fig.3a is below to 180 mAh g^{-1} under the potential range of

3.1.1 Electrochemical behavior and thermal stability of the composite electrodes.

Lithium metal (transition) nitrides with hexagonal symmetry, $P6/mmm$, are composed of M ($M=\text{Co}, \text{Cu}, \text{Ni}$) substituting lithium between the $\text{Li}_2^+\text{N}^{3-}$ layers of Li_3N [5,6]. Fig.1 shows the electrochemical behavior of the lithium transition-metal nitrides prepared from solid-state reaction and high-energy mechanical milling (HEMM). Due to the vacant sites introduced by the doped transition metals, the fully lithiated nitrides can still allow a small amount of lithium intercalation in the first cycle. The compounds gradually undergo an irreversible transformation from a crystalline phase to an amorphous one in the first Li-extraction stage, as shown in Fig.1a. Compared with $\text{Li}_{2.6}\text{Co}_{0.4}\text{N}$, the slight increase of the co-doped nitrides in the charge potentials indicates that part Co substituted by Cu, Ni and Fe may be obstructive to the lithium extraction [7,8]. In the subsequent cycle shown in Fig.1b, the charge potentials become slope and a large amount of lithium can be reversibly re-intercalated and extracted, resulting in high capacities of $700\text{-}950 \text{ mAh g}^{-1}$ which are about 2-3 times over that of the commercial graphite. The discharge potential curves, on the other hand, demonstrate a hysteresis of ca. 0.5 V compared with the charge ones, indicating the different electrochemical kinetics for Li intercalation and extraction. A comparison with $\text{Li}_{2.6}\text{Co}_{0.4}\text{N}$ in the cycling performance reveals that the co-doped compounds have a remarkably enhanced cyclability shown in Fig.2. The significant improvement in the cycling performance for the co-doped nitrides can be attributed to the improved structural stability in association with the Li extraction degree and the enhanced interfacial compatibility [7,8]. Lithium metal nitrides are very attractive in the packing density and volumetric capacity due to the density similar to the current graphite. A major hindrance to the nitrides as promising anode alternatives for graphite is that they possess Li-rich structure and therefore cannot directly combine with the typically high-potential cathodes such as LiCoO_2 and LiMn_2O_4 to constitute Li-ion cells. This deterrent can be overcome by introducing an appropriate amount of Co_3O_4 into the electrodes containing above lithium metal nitrides.

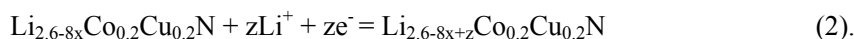
Fig.3 shows charge and discharge curves of the a) Co_3O_4 , b) $\text{Li}_{2.6}\text{Co}_{0.2}\text{Cu}_{0.2}\text{N}$ and c) $\text{Co}_3\text{O}_4\text{-Li}_{2.6}\text{Co}_{0.2}\text{Cu}_{0.2}\text{N}$ based electrodes vs. lithium

0-1.4V. This is attributed that this material has to be electrochemically activated under a very wide potential as 0-3 V [9]. The electrochemical behavior of the $\text{Li}_{2.6}\text{Co}_{0.2}\text{Cu}_{0.2}\text{N}$, which has a high extraction capacity as 800 mAh g^{-1} with a potential plateau of 1.0 V but an insertion capacity low as 230 mAhg^{-1} , is obviously in contrast to that of the Co_3O_4 , as shown in Fig.3b. In the case of $\text{Li}_{2.6}\text{Co}_{0.2}\text{Cu}_{0.2}\text{N}$ plus Co_3O_4 , a very high first charge recovery of ca. 100% shown in Fig3c is remarkable while the cycling is started from an insertion process. Moreover, the composite electrode does not show an obvious potential plateau in the charge stage that reflects the coexistence of two phases in the active hosts similar to that of the $\text{Li}_{2.6}\text{Co}_{0.2}\text{Cu}_{0.2}\text{N}$. Thus, it comes to conclusion that $\text{Li}_{2.6}\text{Co}_{0.2}\text{Cu}_{0.2}\text{N}$ in the composite electrode might be discharged from a delithiated or an amorphous state. The Li-intercalation potential of Co_3O_4 (ca.1.1V) is slightly higher than the Li-extraction potential of lithium metal nitride (ca.1.0V); therefore Co_3O_4 can thermodynamically extract lithium from the nitrides. XRD measurements confirm this point because lithium transfer into Co_3O_4 would be evidenced by a change in the peak intensities for both the hosts. We proposed the reaction mechanism of the composite electrode as follows: $\text{Li}_{2.6}\text{Co}_{0.2}\text{Cu}_{0.2}\text{N} + x\text{Co}_3\text{O}_4 \rightarrow \text{Li}_{2.6-8x}\text{Co}_{0.2}\text{Cu}_{0.2}\text{N} + 4x\text{Li}_2\text{O} + 3x\text{Co}$ (1)



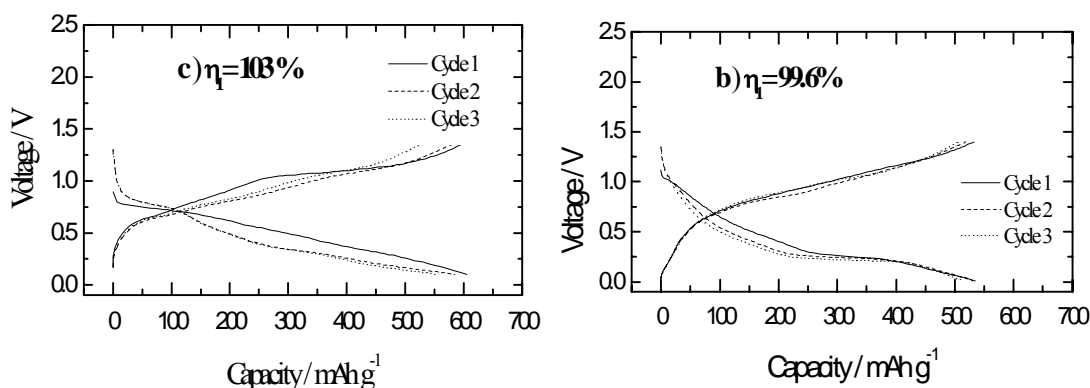
(Left) Fig.3. Charge and discharge curves of different cells based on a) Co_3O_4 , b) $\text{Li}_{2.6}\text{Co}_{0.2}\text{Cu}_{0.2}\text{N}$ and c) $\text{Co}_3\text{O}_4-\text{Li}_{2.6}\text{Co}_{0.2}\text{Cu}_{0.2}\text{N}$, voltage cutoff: 0-1.4 V, vs. Li/Li^+ . Electrode compositions: a) 80 wt.% Co_3O_4 , 10 wt.% AB and 10 wt.% PVDF; b) 70 wt.% $\text{Li}_{2.6}\text{Co}_{0.2}\text{Cu}_{0.2}\text{N}$, 20 wt.% AB and 10 wt.% PVDF and c) 50 wt.% $\text{Li}_{2.6}\text{Co}_{0.2}\text{Cu}_{0.2}\text{N}$, 30 wt % Co_3O_4 , 10 wt.% AB and 10 wt.% PVDF.

(Right) Fig.4. Cyclic voltammogram of the electrode based on a) Co_3O_4 , b) $\text{Li}_{2.6}\text{Co}_{0.2}\text{Cu}_{0.2}\text{N}$ and c) $\text{Co}_3\text{O}_4-\text{Li}_{2.6}\text{Co}_{0.2}\text{Cu}_{0.2}\text{N}$ at the scan rate of 0.05 mV S^{-1} , voltage cutoff: 1.4-0. V, vs. Li/Li^+ . Electrode composites are the same as in Fig.3.



Reaction (1) is a chemical reaction and reaction (2) is an electrochemical one. If $\text{Li}_{2.6-8x}\text{Co}_{0.2}\text{Cu}_{0.2}\text{N}$ is the composition of the fully charged state, then reaction (2) becomes reversible during charge and discharge even at the first cycle. From the experimental results shown in Fig. 3, we estimated x and z as 0.16 and 1.7, respectively. These values correspond to 60/40 weight ratio of $\text{Li}_{2.6-8x}\text{Co}_{0.2}\text{Cu}_{0.2}\text{N}/\text{Co}_3\text{O}_4$ and the reversible capacity of 477 mAh g^{-1} . The capacity was calculated by including $\text{Li}_{2.6-x}\text{Co}_{0.2}\text{Cu}_{0.2}\text{N}$ and Co_3O_4 as active hosts. We observed a first charge efficiency of 100% and a reversible capacity of ca. 520 mAh g^{-1} for the composite electrode containing of 62.5 wt. % $\text{Li}_{2.6-x}\text{Co}_{0.2}\text{Cu}_{0.2}\text{N}$ plus 37.5 wt % Co_3O_4 , as shown in Fig. 3c. The high first cycle efficiency proposed can greatly extend the capacity utilization for the cathode. It is very remarkable because the low charge efficiency of the anodes in the first cycle might consume extra capacity from cathodes and thereby

inevitably reduce the total energy density of the cells. Cyclic voltammogram was further conducted on the electrodes based on different active hosts with a scan rate of 0.05 mV s^{-1} in the potential scale of 0-1.4 V vs. Li/Li^+ , as shown in Fig.5. There is one cathodic peak at about 0.95 V in the first Li-insertion process for Co_3O_4 (Fig.4a. However, this peak does not repeat in the subsequent cycle, indicating that Co_3O_4 turns into inert to lithium. In the case of $\text{Li}_{2.6}\text{Co}_{0.2}\text{Cu}_{0.2}\text{N}$, an obvious anodic peak shown in Fig.4b appears at 1.2 V in the first cycle that corresponds to the two-phase transformation. In the subsequent cycle, one cathodic peak at 0.18 V and two anodic peaks at 0.78, 1.12 V become visible and remain to be stable. However, the large hysteresis in the cathodic and anodic processes seems a drawback and has to be further conquered. In comparison with $\text{Li}_{2.6}\text{Co}_{0.2}\text{Cu}_{0.2}\text{N}$ and Co_3O_4 , obviously, the behavior of the composite electrode shown in Fig.4c is highly consistent with that of $\text{Li}_{2.6}\text{Co}_{0.2}\text{Cu}_{0.2}\text{N}$, suggesting that the active host in the composite is mainly associated with lithium metal nitrides. Furthermore, a weak cathodic peak at 0.95 V corresponding to the Co_3O_4 indicates that the thermodynamically spontaneous reaction may not entirely drive lithium into the Co_3O_4 before the electrochemical cycling. The composite electrodes demonstrated high cycling stability, due to that they could be benefited from the low volume effects of the lithium metal nitrides upon Li insertion and extraction. As measurement, the charge yield of the composite electrode during cycling is always at 100%, indicating that Co_3O_4 remains inactive and stable in the electrode while lithium in the nitrides can be electrochemically intercalated and extracted with high reversibility under a suitable potential window. The composite electrode consisting of $\text{Li}_{2.6-x}\text{Co}_{0.2}\text{Cu}_{0.2}\text{N}-\text{Co}_3\text{O}_4$ was found to show good electrochemical behavior with the solid PEO electrolytes. A high charge efficiency of 99.6 % and a large capacity of 520 mAh g^{-1} shown in Fig.5 become feasible, indicating that lithium can be electrochemically



(Left) Fig.5. Charge and discharge profiles of the SnSb- $\text{Li}_{2.6}\text{Co}_{0.4}\text{N}$ electrode with PEO at 65°C .

(Right) Fig.6. Charge and discharge profiles of the Co_3O_4 - $\text{Li}_{2.6}\text{Co}_{0.2}\text{Cu}_{0.2}\text{N}$ electrode with PEO at 65°C .

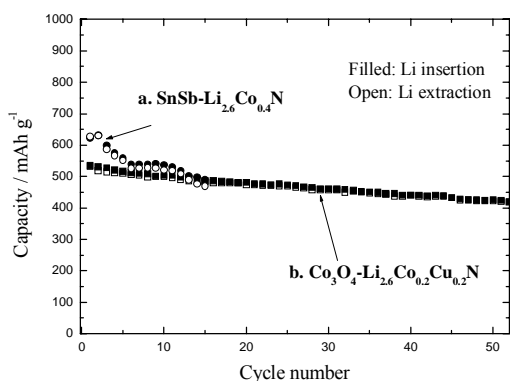


Fig.7. Cycling performance of the composite anodes with PEO electrolytes.

intercalated into and extracted from the nitrides with high reversibility while operating with the PEO electrolytes.

On the other hand, the composite electrode based on SnSb and $\text{Li}_{2.6}\text{Co}_{0.4}\text{N}$ also demonstrates a high first charge efficiency of 103 %, which is attributed to the fact that lithium metal nitrides can make a capacity compensation for the ultrafine alloy hosts in the first cycle [10]. As can be seen, the charge-discharge behavior of the SnSb- $\text{Li}_{2.6}\text{Co}_{0.4}\text{N}$ composite electrode reflects the mixing electrochemical characteristics of these two types of active hosts, as shown in Fig.6. The capacity changes, as a function of cycling, for different anodes with the solid PEO electrolytes are shown in Fig. 7. The SnSb- $\text{Li}_{2.6}\text{Co}_{0.4}\text{N}$ anode has a large capacity of over 600 mAh g^{-1} in the cycling beginning. However, a gradual deterioration in the cycling performance is always observed. A replacement of $\text{Li}_{2.6}\text{Co}_{0.4}\text{N}$ with the

co-doped nitrides proposed does not bring any progress, indicating that the volume effect from the Li-alloying reaction possesses a morphological instability at the interface while operating with the solid-state PEO electrolytes.

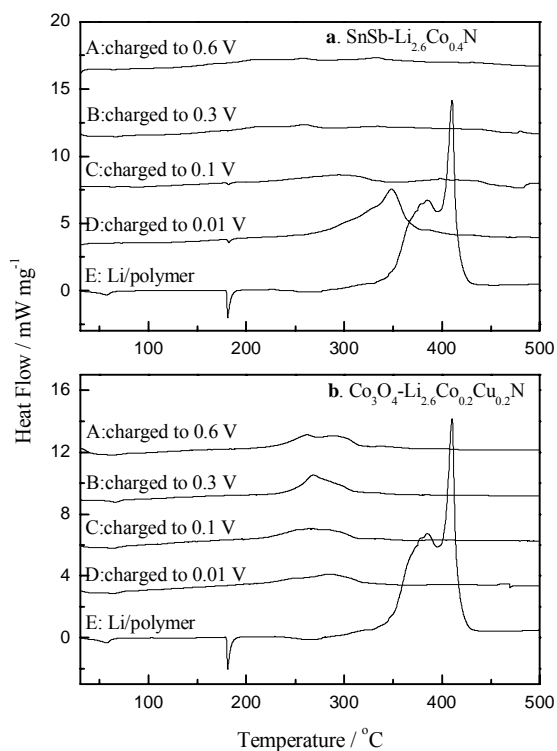


Fig.8. DSC curves of the composite anodes of a) SnSb- $\text{Li}_{2.6}\text{Co}_{0.4}\text{N}$ and b) $\text{Li}_{2.6}\text{Co}_{0.2}\text{Cu}_{0.2}\text{N}-\text{Co}_3\text{O}_4$ with various Li intercalation states (Heating rate: $5^\circ\text{C}/\text{min}$).

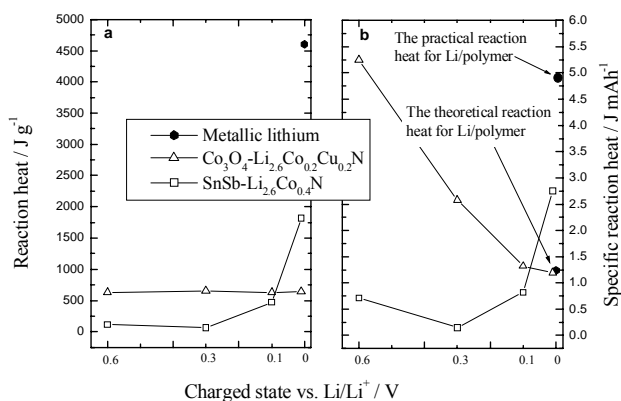


Fig.9. Reaction heat vs. charged state by a) J g^{-1} and b) J mAh^{-1} for different anodes at 65

Fig.10 further shows the typical charge and discharge profiles of the full cells based on the $\text{LiNi}_{0.8}\text{Co}_{0.2}\text{O}_2$ cathode and the different anodes of lithium metal, SnSb- $\text{Li}_{2.6}\text{Co}_{0.4}\text{N}$ and $\text{Li}_{2.6}\text{Co}_{0.2}\text{Cu}_{0.2}\text{N}-\text{Co}_3\text{O}_4$, respectively, while operating with the PEO electrolytes at 65 . The $\text{LiNi}_{0.8}\text{Co}_{0.2}\text{O}_2/\text{Li}$ cell demonstrates a high working potential of 3.5-4.0 V with a capacity of 120 mAh g^{-1} , as shown in Fig.10a. Replacing the lithium metal with the insertion anodes could result into a loss in the working potential but an improvement in the safety. In general, for full utilization of lithium storage capacity of the composite anodes, the weight of cathodes has to be much over that of anodes at about 4~5 times. As can be seen from Fig.10b, the high similarity in the potential-capacity trends for the $\text{LiNi}_{0.8}\text{Co}_{0.2}\text{O}_2/\text{Li}_{2.6}\text{Co}_{0.2}\text{Cu}_{0.2}\text{N}-\text{Co}_3\text{O}_4$ cell indicates that the amorphous lithium metal nitrides remain high

By using the $\text{Li}_{2.6-x}\text{Co}_{0.2}\text{Cu}_{0.2}\text{N}-\text{Co}_3\text{O}_4$ anode, a significantly improved cycling performance was obtained with a high capacity of 500 mAh g^{-1} . The charge-discharge efficiency is almost 100% and the capacity fade during cycling is estimated to be only about 0.37%/cycle. The capacity retention can be further improved by decreasing moisture in the PEO electrolytes since hexagonal lithium metal nitrides suffer from a high sensitivity with H_2O .

The safety of small size lithium-ion cells under normal use is well established. In contrast, the safety of the large size lithium-ion batteries is still questionable, especially in cases of abusive use. Safety of lithium ion batteries is mainly related to the thermal reactivity of the components. Fig.8 shows differential scanning calorimetric curves (DSC) for the composite anodes of $\text{Li}_{2.6}\text{Co}_{0.4}\text{N}-\text{SnSb}$ (a) and $\text{Li}_{2.6}\text{Co}_{0.2}\text{Cu}_{0.2}\text{N}-\text{Co}_3\text{O}_4$ (b) with the PEO electrolytes, respectively, as a function of the charged state along with that for Li metal with the PEO electrolytes (1:1 weight ratio) as a reference. For the $\text{Li}_{2.6}\text{Co}_{0.4}\text{N}-\text{SnSb}$ anode, the reaction heat strongly depends on the charged state. The reaction heat is very low for the composite anode charged up to 0.3 V and appreciable for that charged up to 0.1 V, as shown in Fig.8a. An endothermic peak in the anode charged to 0.1 V is observed at 180°C in the DSC curve, which corresponds to the fusion of lithium metal. That is, the high level insertion of lithium into the $\text{Li}_{2.6}\text{Co}_{0.4}\text{N}-\text{SnSb}$ composite exhibits a lithium metal deposition. On the other hand, the reaction heat of the $\text{Li}_{2.6}\text{Co}_{0.2}\text{Cu}_{0.2}\text{N}-\text{Co}_3\text{O}_4$ anode shows exothermic peaks at $250\sim 320^\circ\text{C}$, which do not depend on the charged state, as shown in Fig.8b. Fig.9 shows the reaction heat (a) and specific reaction heat (b) of the different anodes at various charged states. The reaction heat of the anode should be compared in terms of energy per discharged capacity, i.e., J mAh^{-1} (a specific reaction heat). Specific reaction heats for the $\text{Li}_{2.6}\text{Co}_{0.2}\text{N}-\text{SnSb}$ anode charged up to 0.1V vs. Li/Li^+ and 0.01 V vs. Li/Li^+ are 0.82 J mAh^{-1} and 2.75 J mAh^{-1} , respectively. Those for the $\text{Li}_{2.6}\text{Co}_{0.2}\text{Cu}_{0.2}\text{N}-\text{Co}_3\text{O}_4$ anode are estimated to be 1.1 J mAh^{-1} compared to that of 1.24 J mAh^{-1} in lithium metal and PEO electrolyte (1:1 weight ratio). In practice, in the case of a lithium metal anode, an excess amount of lithium metal, at least four times compared to the cathode capacity, should be used because of the dendrite formation on the anode. Therefore, the reaction heat could be estimated to reach 4.96 J mAh^{-1} or higher.

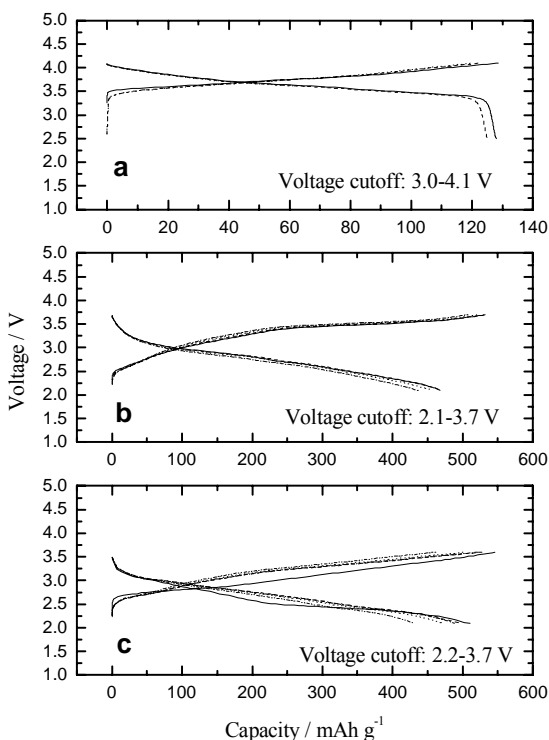
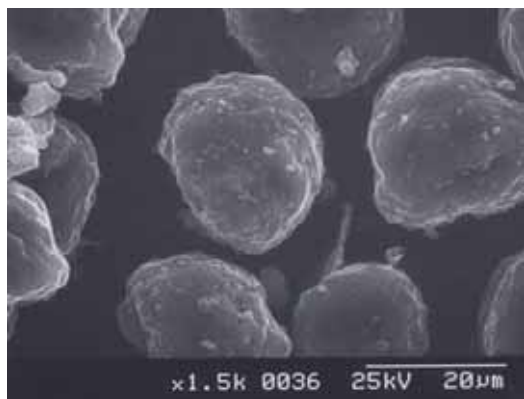


Fig.10. Charge and discharge profiles of the full cells based on $\text{LiNi}_{0.8}\text{Co}_{0.2}\text{O}_2$ cathode and anode of a) Li, b) $\text{Co}_3\text{O}_4\text{-Li}_{2.6}\text{Co}_{0.2}\text{Cu}_{0.2}\text{N}$ and c) $\text{SnSb-Li}_{2.6}\text{Co}_{0.4}\text{N}$. Electrode compositions of b) and c) are the same as in Fig.9.

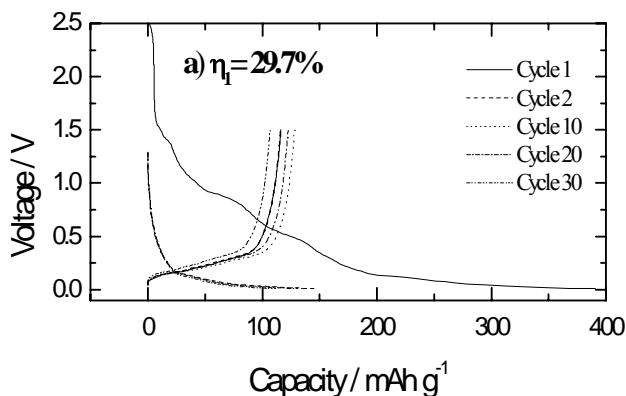


(Left) Fig.11 SEM images of the MCMB particles.

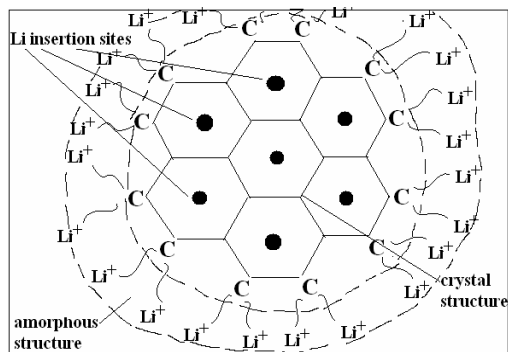
stability from cycle to cycle. On the other hand, the voltage plateau of the $\text{LiNi}_{0.8}\text{Co}_{0.2}\text{O}_2/\text{SnSb-Li}_{2.6}\text{Co}_{0.4}\text{N}$ cell slightly increases from the first to the following cycles, which probably is attributed to the two-phase transformation of $\text{Li}_{2.6}\text{Co}_{0.4}\text{N}$ between the crystal and the amorphous, as shown in Fig.10c. The high initial coulombic efficiency of over 95 % and the large reversible anode capacity above 450 mAh g^{-1} are very remarkable for both the composite anodes, which might be highly favorable for realizing a rather high energy density and can be considered as an ideal power source for HEV & EV. However, bearing in mind that the morphological instability from the Li-alloy host is still questionable, continuous research would be pursued to develop the lithium metal nitrides- Co_3O_4 based composite electrodes proposed with low volume effects.

3.1.2 Modified graphitic carbon as insertion anodes.

From the application point of view, the first approach for lithium metal-free anode is to use graphite, as is accomplished in lithium-ion batteries with organic solvent electrolytes. The charge and discharge profile of mesocarbon microbead (MCMB, morphology as shown in Fig.11), a typical graphitic carbon used in the current lithium-ion cells, is shown in Fig.12. The very low charge efficiency of 29.7 % in the first cycle indicates that side reactions occur both in the reduction and oxidation processes which lead to some uncertainty in the determination of the maximum reversible capacity of the graphitic carbon. Consequently, its reversible capacity is



(Right) Fig.12. Charge and discharge profiles of the MCMB electrode with PEO electrolytes at 70



below to 150 mAh g^{-1} and the charge and discharge efficiency in the first several cycles is extremely low. Poor solid/solid interface of the graphite with the PEO electrolytes indicates that structural and interfacial performance has to be improved.

To make the graphitic carbon operate well with PEO electrolytes, we design an ionic conducting LiC_x layers by directly reacting the opened C-atom with lithium under special conditions (such as high pressure and low temperature) on the surface of the graphitic carbon that can prevent the side reaction

Fig.13. Structural images of the modified graphitic carbon.

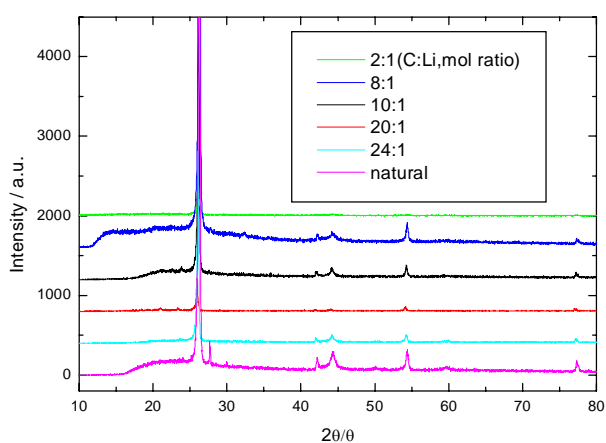


Fig.14 XRD of the modified MCMB under different Li/C ratio.

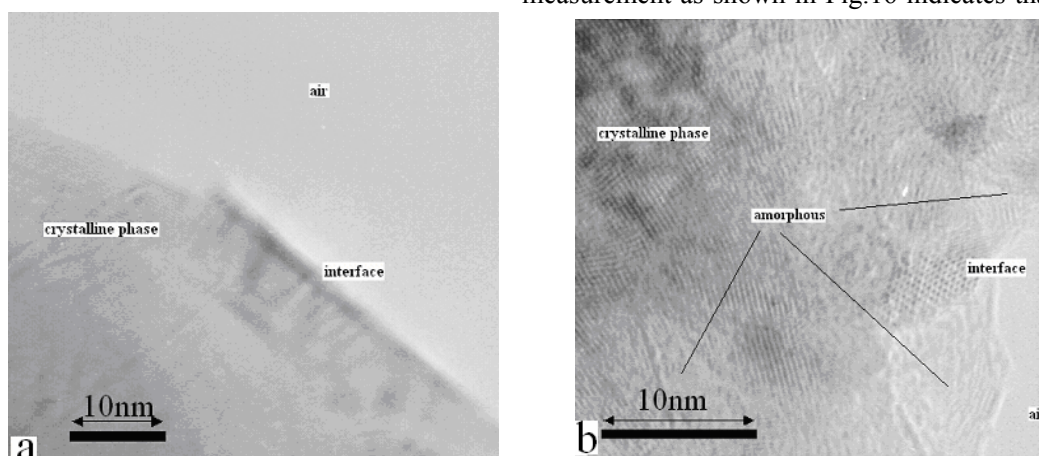


Fig.15. TEM images on the surface of the MCMB at left) without modification and right) after modification.

irreversible reaction in the first cycle is highly suppressed after the treatment, which is favorable for the electrochemical kinetics during lithium insertion into and extraction from the layered carbon. Finally, Fig.17 shows that the modified MCMB with PEO electrolytes presents an attractive behavior similar to that based on the common liquid electrolytes. Li intercalation into the graphitic hosts possesses several stages below to 200 mV. However, in the real battery testing, only one potential plateau between 0.2-0 V can be distinguished, which is correspond to the LiC_x compound reaction in an equilibrium phase. The capacity as a function upon the cycles also demonstrates high stability, as shown in Fig.18. The reversible capacity is measured to be about 290 mAh g^{-1} , which is very comparable and close to the theory data (LiC_6). Furthermore, we compared the thermal stability of the MCMB with metallic lithium while operating with the PEO electrolytes via DSC measurement, as shown in Fig.19. MCMB shows very low reaction heat under high Li utilization with the PEO electrolytes in comparison with lithium metal anode. Such a thermal behavior is highly opposite to the one based on liquid electrolytes, in which the heat generation of graphite is very significant, especially, that of the reaction heat of PVDF and LiC_x [11]. This result indicates that graphitic carbon might be a suitable anode candidate in large size rechargeable lithium-ion batteries based on PEO electrolytes for EV in terms of structural stability and thermal reliance stability.

Table.1. XPS results of the MCMB with and without treatment.

		Li _{1s}	C _{1s}	F _{1s}	O _{1s}
Without treatment	Binding energy	0	285 ev,	0	533.00 ev,
	Chemical composition	0	97.81%	0	2.19%
With treatment	Binding energy	56.10 ev,	291 ev,	0	532.80 ev
	Chemical composition	2.23 %	37.50 %	0	60.20 %

in the interface between the electrode and the PEO electrolyte, as shown in Fig.13. Due to high Li-reactivity of its surface, MCMB is chosen and treated by high energy ballmilling with lithium metal by the aid of dodecane ($\{\text{CH}_3(\text{CH}_2)_{10}\text{CH}_3\}$) under Ar. The high energy ballmilling can make the surface of MCMB become disordered and therefore surface C-atom become open and further can react with Li.

Fig.14 shows that the typical crystalline structure of the treated MCMB remains to be unchanged which can permit lithium reversible insertion and extraction. XPS results as shown in Table 1 confirmed the formed LiC_x layer on the graphite surface. TEM observation shown in Fig.15 further reveals that the MCMB loss crystal on its surface upon treatment, indicating that the formed LiC_x is prevailed by amorphous or micro-crystalline phase. Cyclic voltammogram measurement as shown in Fig.16 indicates that the side

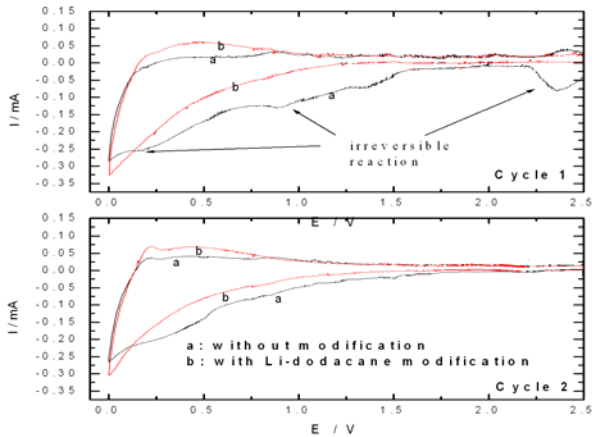


Fig.16. Cyclic voltammogram of the electrode based on a) no modified MCMB, b) $\text{Li}_{2.6}\text{Co}_{0.2}\text{Cu}_{0.2}\text{N}$ and c) $\text{Co}_3\text{O}_4\text{-Li}_{2.6}\text{Co}_{0.2}\text{Cu}_{0.2}\text{N}$ at the scan rate of 0.05 mV S^{-1} , voltage cutoff: 1.4-0. V, vs. Li/Li^+ .

3.2 Cathode

The selection for proper cathodes is according to the following requirements, such as inexpensive, environmentally benign, wide operating temperature, good capacity/cycling performance, extremely safe. Transition metal oxides, such as LiCoO_2 , layered LiNiO_2 and LiMn_2O_4 have found application as positive electrode materials for high power applications. These materials provide high potentials (about 4 V vs. Li) and good reversible capacities (about 120 mA h g^{-1}). The use of LiMn_2O_4 solves problems related to cost and Co and Ni toxicity, but the disproportionation of Mn^{3+} remains a severe problem. Previous research reveals that most of the current cathodes suffers from side reaction with PEO electrolytes and detrimental phase transitions above 70 °C that inevitably cause to capacity loss and fade while being oxidized at a high potential. In this work, in comparison with several cathode materials, such as Li_xCoO_2 ($0.5 < x < 1$, 0.5-electron reaction, $\text{Cap}=137 \text{ mAh g}^{-1}$), $\text{Li}_x\text{Mn}_2\text{O}_4$ ($0 < x < 1$,

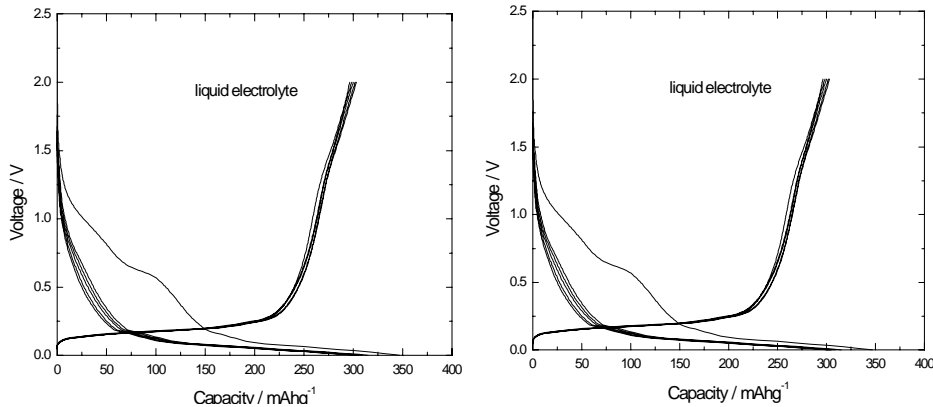
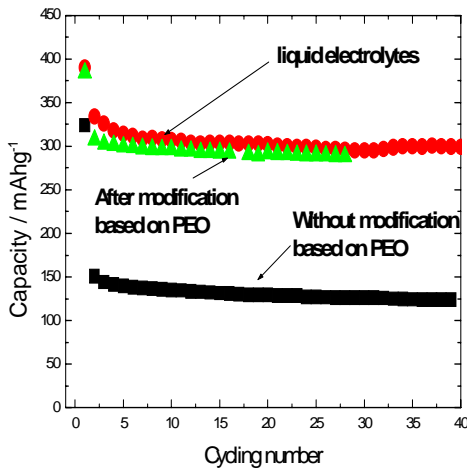
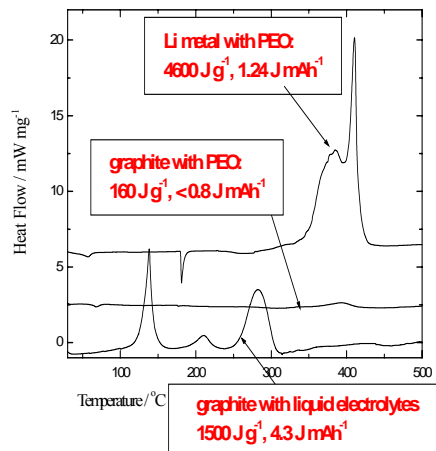


Fig.17. Comparison in the charge and discharge profiles of the MCMB based on liquid electrolytes and the modified MCMB based on PEO electrolytes.



(Left) Fig.18. Cycling performance of different MCMB electrodes with liquid and PEO electrolytes.



(Right) Fig.19. DSC curves of different electrode with PEO and liquid electrolytes.

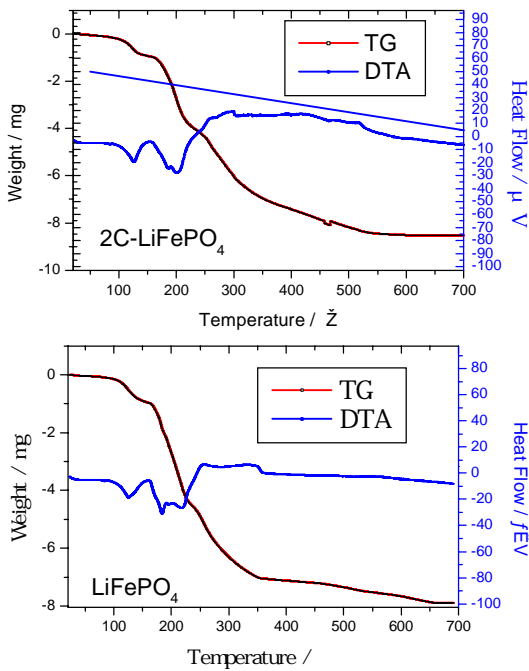


Fig.20. TG/DTA curves of the LiFePO_4 with and without PVC during heating to 700

0.5-electron reaction, $\text{Cap}=148 \text{ mAh g}^{-1}$) and Li_xFePO_4 ($0 < x < 1$, 1-electron reaction, $\text{Cap}=170 \text{ mAh g}^{-1}$), olivine type LiFePO_4 is very attractive due to its capability to operate within a very flat voltage plateau (around 3.5 V), high thermal stability, high working temperature performance similar to PEO electrolytes, low lattice volume changes, low cost and benign environmental properties [12].

However, a significant drawback of the LiFePO_4 is its poor rate capability caused by poor electron conductivity. In this work, we use poly (vinyl chloride) as carbon sources to produce the LiFePO_4/C composite by means of two pyrolysis reactions. The electronic conductivity of the LiFePO_4 can be substantially enhanced by dispersing fine particle size of the active hosts in the carbon matrix. With this modification, the LiFePO_4 is capable of providing high capacity and high charge rates. TG/DTA analysis conducted on the product upon the heating process shown in Fig.20 reveals that the LiFePO_4 possesses several decomposition reaction related to the starting materials. The PVC does not cause to a reaction with the LiFePO_4 . The carbon contents of the LiFePO_4/C was confirmed to be about 5-7.5 wt% with the TG analysis. XRD technique confirms the crystalline structure of the composite proposed, as shown in Fig.21. As well, pyrolyzed carbon that is prevailed with disordered structure can be found in the product. Carbon coating process does not bring a obvious change in the lattice parameters of the LiFePO_4 , as shown in table.2, indicating the thermal pyrolysis mainly causes to a modification in the morphology. The homogeneous distribution of the active hosts within the carbonaceous matrix is further evidenced by the elemental distribution

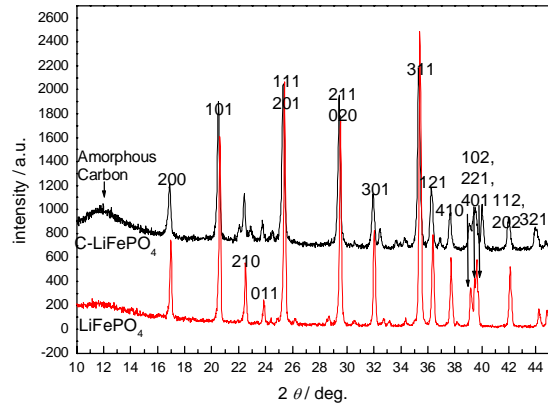


Fig.21. XRD of the resulting LiFePO_4 and LiFePO_4/C powders.

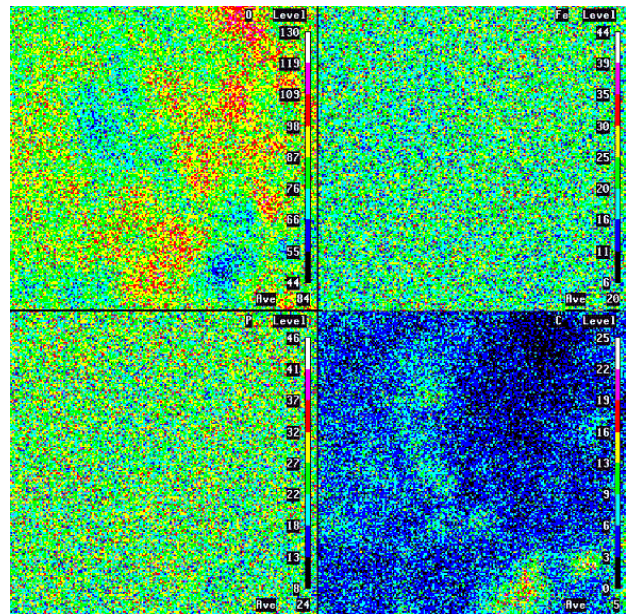


Fig.22. EPMA images of elemental distribution of the resulting materials.

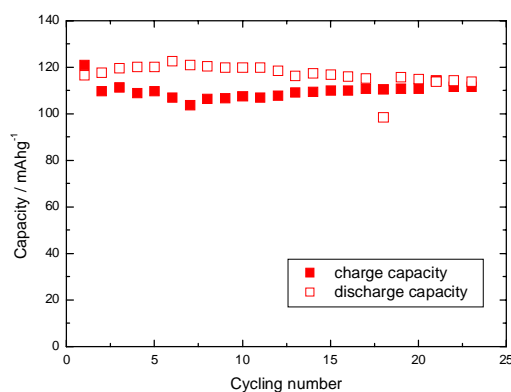
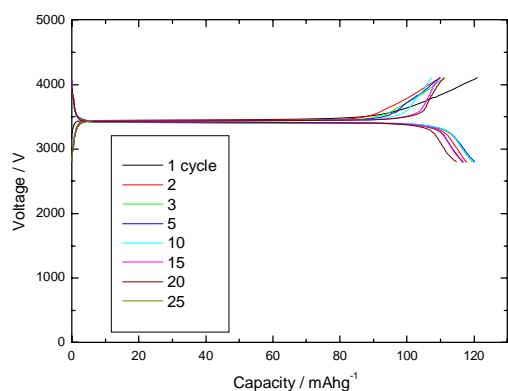


Fig.23. SEM images of the resulting LiFePO_4/C powders.

mapping from Electron Probe Micro-Analysis (EPMA) shown in Fig.22. SEM observation shown in Fig.23 further reveals that the material possesses high porosity which is favorable for increasing the reactive area and therefore the electrochemical kinetics. It suggests that the introduction of highly dispersed PVC has an effect on preventing the single LiFePO_4 growth during heating process. Meanwhile, the possible aggregation of the active hosts during high temperature could be highly barred, resulting in fine grains of the active hosts which favorable for the electrochemical kinetics. Finally, Fig.24 and 25 show that the LiFePO_4/C electrode presents a stable working potential at about 3.5 V vs Li/Li^+ and a capacity of 120 mAh g^{-1} , as well as excellent cycling stability, probably due to the low lattice volume changes with Li insertion/extraction and good interfacial compatibility with the solid PEO electrolytes. The primary results suggest that the modified olivine type LiFePO_4 might be a good cathode candidate for the PEO electrolytes.

Table.2. Lattice parameters of the resulting compounds.

	a-axis	b-axis	c-axis	Cell volume	Crystal structure
LiFePO_4	10.380	6.023	4.714	294.777	Orthorhombic
2C-LiFePO_4	10.381	6.015	4.711	294.203	Orthorhombic



(Left) Fig.24. Typical charge and discharge profiles of LiFePO_4/C with PEO electrolytes at 65°C (2.8-4.1 V).

(Right) Fig.25. Cycling performance of the LiFePO_4/C with PEO electrolytes at 65°C .

4. Conclusions

1) Composite anodes based on hexagonal lithium metal nitrides have been developed to show larger capacity and higher first cycle efficiency over the current graphitic anodes. However, the performance of the composite anodes containing Li-alloy hosts is still in doubt due to that the Li-alloy has a morphological instability along with an increased heating generation dependent on Li-insertion. In contrast, the composite anodes containing lithium transition-metal nitrides and Co_3O_4 demonstrate high first charge efficiency of 100 % and large capacity of 500 mAh g^{-1} , as well as high cycling stability and low reaction heating under high Li-utilization with the PEO electrolytes, indicating that they possess potential applications in large size rechargeable lithium-ion batteries for EV in terms of high first-cycle charge efficiency, large capacity and high thermal reliance;

2) Graphitic carbon that is currently used in commercial Li-ion batteries can be successfully operated with the PEO electrolytes by designing an amorphous LiC_x layer on its surface which can prevent the side reaction. The material treating process is effective and comparable in production. The modified graphitic carbon demonstrates good electrochemical behavior similar to that in liquid electrolytes. Furthermore, high thermal stability of the graphitic carbon with PEO electrolytes under deep Li utilization suggests that the graphitic carbon might be suitable anode candidates in large size rechargeable lithium-ion batteries for EV based on PEO electrolytes in terms of structural stability and thermal reliance;

3) LiFePO_4/C composite has been prepared by two pyrolysis processes using poly (vinyl chloride) as carbon sources. The material was confirmed to be of high porosity and homogeneous distribution of active hosts within the carbonaceous matrix. Primarily electrochemical results indicate that the olivine type LiFePO_4/C is a promising cathode candidate in terms of stable working potential, acceptable capacity, high charge/discharge efficiency and excellent cycle life with the PEO electrolytes at the elevated temperature.

References

- [1] Y. Aihara, M. Kodama, K. Nakahara, H. Okise, K. Murata, *J. Power Sources* 65, 143 (1997).
- [2] M.D. Farrington, *J. Power Sources* 96, 260 (2001).
- [3] D. Fauteux and R. Koksang, *J. Appl. Electrochem.* 23, 1 (1993)
- [4] J. O. Besenhard, J. Yang and M. Winter, *J. Power Sources* 68, 87 (1997)
- [5] M. Nishijima, T. Kagohashi, N. Imanishi, Y. Takeda, O. Yamamoto and S. Kondo, *Solid State Ionics*, 83, 107 (1996).
- [6] M. Nishijima, T. Kagohashi, N. Imanishi, Y. Takeda, O. Yamamoto, *J. Power Sources*, 68, 510 (1996).
- [7] Y. Liu, K. Horikawa, M. Fujiyosi, N. Imanishi, A. Hirano and Y. Takeda, *J. Electrochem. Soc.*, 151, A1450 (2004).
- [8] Y. Liu, T. Matsumura, N. Imanishi, T. Ichikawa, A. Hirano, Y. Takeda, *Electrochemistry Communications*, 6, 632 (2004).
- [9] P. Poizot, S. Laruelle, S. Grugeon, L. Dupont, J-M. Tarascon, *Nature*, 407, 496 (2000).
- [10] J. Yang, Y. Takeda, N. Imanishi and O. Yamamoto, *J. Electrochem. Soc.*, 147, 1671 (2000)
- [11] Ph. Biensan, B. Simon, J.P. Peres, A.de. Guiber, M. Broussely, J.M. Bodet and F. Pertont, *J. Power Sources*, 81-82, 906 (1999).
- [12] A.K. Padhi, K.S. Nanjundaswamy, J.B. Goodenough, *J. Electrochem. Soc.* 144 (1997) 1188